ARTICLES
https://doi.org/10.1038/s41558-018-0391-7
nature climate change

Organic matter from Arctic sea-ice loss alters bacterial community structure and function

Graham J. C. Underwood[1,7*], Christine Michel[2,7], Guillaume Meisterhans[2], Andrea Niemi[2], Claude Belzile[3], Matthias Witt[4], Alex J. Dumbrell[1] and Boris P. Koch[5,6]

Continuing losses of multi-year sea ice (MYI) across the Arctic are causing first-year sea ice (FYI) to dominate the Arctic ice pack. Melting FYI provides a strong seasonal pulse of dissolved organic matter (DOM) into surface waters; however, the biological impact of this DOM input is unknown. Here we show that DOM additions cause important and contrasting changes in under-ice bacterioplankton abundance, production and species composition. Utilization of DOM was influenced by molecular size, with 10–100 kDa and >100 kDa DOM fractions promoting rapid growth of particular taxa, while uptake of sulfur and nitrogen-rich low molecular weight organic compounds shifted bacterial community composition. These results demonstrate the ecological impacts of DOM released from melting FYI, with wide-ranging consequences for the cycling of organic matter across regions of the Arctic Ocean transitioning from multi-year to seasonal sea ice as the climate continues to warm.

The Arctic is undergoing accelerated warming[1], resulting in changes to the areal extent and age profile of sea ice. Thick ice that persisted over multiple years (MYI) is being replaced by thinner seasonal FYI[2–4], significantly changing the ecology and biogeochemistry of the Arctic Ocean[5,6]. FYI hosts productive microbial assemblages that accumulate large amounts of DOM[7–10], and supports important ice-associated food webs[11]. Increased seasonal melting of FYI and the predicted complete shift from MYI to FYI in the Arctic[12], and important differences in richness and diversity between MYI, FYI and underlying seawater bacterial communities[13,14], suggests that under-ice microbial communities may be affected by sea-ice DOM inputs, although rates of utilization and degree of selectivity by bacterial planktonic assemblages are still to be determined. Determining the cycling and role of the ice-derived DOM pool in affecting water column microbial assemblages will improve our understanding of biogeochemical cycling in an Arctic significantly altered by climate change.

DOM influences the physical structure of sea ice[7,8], with organic matter held within brine channels in various molecular size configurations (a continuum of dissolved, colloids and gels[10,15,16].) These substances are released into the surface waters on ice melt[6,17,18]. Differential retention of dissolved and gel organic fractions in ice means that organic fluxes vary during the melt period[18,19]. Concentrations of dissolved organic carbon (DOC) at the time of ice melt in surface waters can be high: >250 µmol l^{-1} in under-ice surface waters of the Canadian Archipelago and the Beaufort Sea[20–22] and 300 µmol l^{-1} near Barrow, Alaska[19]. However, the fate of these DOM constituents once released into the under-ice surface water remains an open question. In the seasonally stratified under-ice water column, ice-derived DOM is utilized by bacterioplankton, contributing to its biogeochemical cycling during the early-ice melt period[6,23,24] and also to carbon burial[25] and aerosol formation[26]. Bacterioplankton off Svalbard derives 59% of their carbon requirements from ice-algal carbon, despite other carbon sources being available[27]. Sea-ice DOM also has a priming effect, enhancing the degradation of riverine DOM in seawater[28], emphasizing the important seasonal role of DOM release from sea ice in microbial biogeochemical cycling in Arctic surface waters[6,11].

We tested the hypothesis that addition of different Arctic sea-ice DOM fractions at concentrations similar to those measured under ice during ice melt would alter the diversity and structure of the under-ice bacterioplankton community and influence carbon turnover of different organic constituents. We isolated fresh sea-ice DOM from the algal-rich bottom layer of FYI. This layer contains over 90% of the algal biomass in the ice profile[29] and high concentrations of DOM, containing a spectrum of molecular size classes, including extracellular polymeric substances (EPS) produced by sea-ice diatoms[9,10,30,31]. Using differential molecular weight filtering, we obtained three fractions: (1) sea-ice-derived DOM filtered through glass fibre filters (GF/F) (termed 'DOMtot' in the following); (2) a high molecular weight (HMW) DOM fraction retained on a 100 kDa filter and (3) a low molecular weight (LMW) fraction retained between 10 kDa and 100 kDa filters. These three fractions were added to independent replicate microcosms containing natural under-ice seawater (30 per treatment) incubated at in situ temperatures. We followed microbial community responses over 9 days in terms of substrate utilization, bacterial growth and changes in taxonomic composition, determined by next-generation sequencing (NGS) (Ion Personal Genome Machine (PGM) and 454) of 16S ribosomal RNA genes. We applied solid-phase extraction followed by ultrahigh resolution Fourier transform-ion cyclotron resonance-mass spectrometry (FT-ICR-MS) to characterize the changes in elemental composition and utilization of DOM of the treatments. The analytical window for this characterization covered molecular masses from 200 to 600 Da[32].

Results and Discussion

Under-ice seawater contained 60 µmol l^{-1} DOC, as previously reported for Arctic waters[24,33]. DOMtot, HMW and LMW additions significantly increased DOC concentrations, compared to controls

[1]School of Biological Sciences, University of Essex, Colchester, UK. [2]Fisheries and Oceans Canada, Freshwater Institute, Winnipeg, Manitoba, Canada. [3]Institut des Sciences de la Mer de Rimouski, Université du Québec à Rimouski, Rimouski, Quebec, Canada. [4]Bruker Daltonik GmbH, Bremen, Germany. [5]Alfred-Wegener-Institut Helmholtz-Zentrum für Polar- und Meeresforschung, Bremerhaven, Germany. [6]University of Applied Sciences, Bremerhaven, Germany. [7]These authors contributed equally: Graham J. C. Underwood, Christine Michel. *e-mail: gjcu@essex.ac.uk

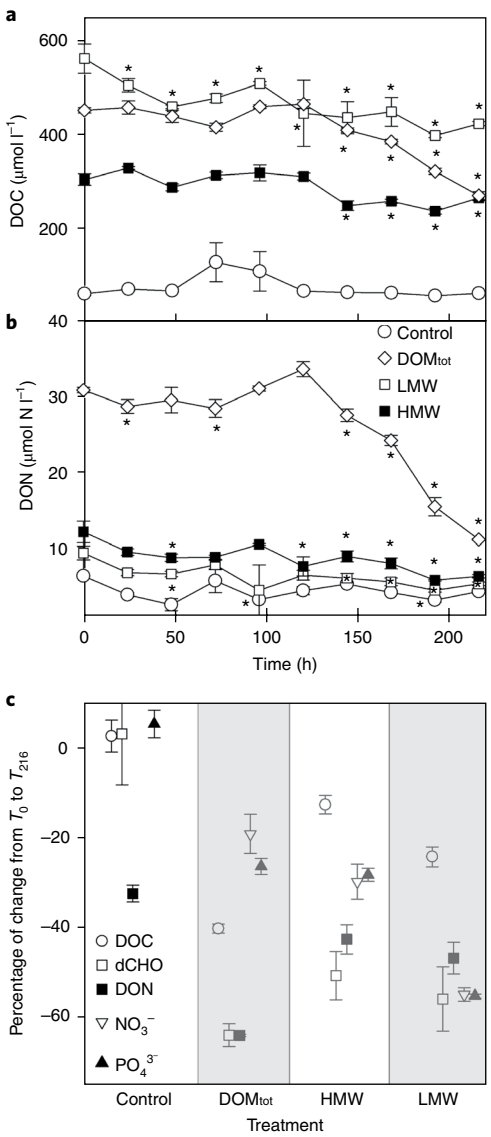

Fig. 1 | Changes in concentrations of dissolved organic and inorganic components during experiments of Arctic under-ice surface water enriched with three sea-ice-derived organic matter fractions (DOM, LMW and HMW). a, DOC concentration. **b**, DON concentration. **c,** Percentage utilization of dissolved organic and inorganic carbon, nitrogen and phosphorus components (comparing time; T_0 to T_{216} hours). NO_3^- nitrate; PO_4^{3-} phosphate; mean ± s.e.m., $n = 3$; the asterisk denotes samples significantly different (analysis of variance (ANOVA) $P < 0.01$ or less) from T_0 concentration.

(Fig. 1a and Supplementary Table 1), to values within the range of DOC measured under sea ice during ice melt[19–22,24]. The treatments contained higher concentrations of DOM than in enrichment studies using MYI[17] due to the higher diatom-dominated algal biomass and the predominance of diatom-derived DOM and EPS in the bottom layers of FYI at this site and in the Canadian Archipelago[10,29,34,35]. In the DOMtot addition, DOC and dissolved carbohydrates (dCHO) had similar enrichment factors, whereas DOC enrichment was greater than that of dCHO in the HMW and LMW additions (Supplementary Table 1). Up to 68% of the dCHO in bottom-ice is <8 kDa[10], which was not preferentially retained by the molecular filters in both HMW and LMW treatments. LMW (<600 Da) solid-phase extractable organic compounds were present in all four treatments, and their molecular formulas were identified using FT-ICR-MS (Supplementary Fig. 2). The <600 Da sea-ice DOMtot fraction included a large number of unique formulas (Supplementary Table 1), in particular compounds with higher hydrogen/carbon (H/C) and carbon/nitrogen (C/N) but lower oxygen/carbon (O/C) and carbon/sulfur (C/S) ratios, compared to the background seawater DOM (Supplementary Fig. 2, Table 1 and Supplementary Table 1). The HMW and LMW additions altered the molecular formula composition of the <600 Da fraction, with unique compounds added in both treatments. We assume that these smaller monomers can form intermolecular aggregates[15,36] that are retained by membrane-based separation techniques and are therefore present in the added material. Key differences in the organic matter profiles between the DOMtot, HMW and LMW treatments were a greater proportion of EPS-carbohydrate (16–24% of dCHO, Supplementary Table 1), and higher DOC/DON (dissolved organic nitrogen) ratios (Supplementary Fig. 1) in the HMW and LMW additions. This shows that these molecular filter cut-offs retained the EPS produced by ice diatoms[10,31], which are the dominant autotrophs in FYI in our study region[10,37,38]. DOMtot additions showed higher concentrations of dCHO (but a lower percentage contribution of HMW EPS constituents), higher numbers of unique molecular formulas <600 Da and higher DON concentrations (Fig. 1b and Supplementary Table 1). The different additions provided a range of DOM sources, encompassing the spectrum described by the size–reactivity continuum model[16]. These sources had a variety of different chemical constituents, potentially selecting for different bacterial taxa[39–41].

Concentrations of DOC, DON and dCHO decreased significantly in the addition treatments over 9 days (216 h; Fig. 1a,b and Supplementary Fig. 1a), with differences in the amount of organic and inorganic components utilized. There were no significant changes in concentrations in the controls (Fig. 1c and Table 1). Proportionally more dCHO (50–60%) was utilized compared to the overall utilization of DOC (between 13% and 40%), including in the HMW and LMW treatments (Fig. 1c), despite the carbohydrate enrichment in these treatments being lower than the overall DOC enhancement (Supplementary Table 1). This indicates that bacterial growth responses were not affected solely by DOM concentration, but also DOM composition. In the HMW and LMW additions, bacterioplankton used nitrate as well as DON (Fig. 1c and Supplementary Fig. 3a). Assimilation of inorganic nitrogen sources was also observed in studies where carbohydrates or mono-sugars were preferentially used for growth[16,17]. However, in the DOMtot addition, there was substantial utilization of DON in preference to nitrate (Fig. 1b,c and Table 1). A similar level of utilization of DON by Arctic bacterioplankton was observed in addition experiments using riverine DOM[42]. DOC/DON ratios increased with time, with the HMW and LMW treatments showing the greatest increases (Supplementary Fig. 1b).

There were no significant differences in bacterial density at T_0 between treatments and controls (Fig. 2). HMW and LMW additions stimulated logarithmic bacterial growth, with peak bacterial production occurring from 144 to 216 h (Fig. 2a,b) and intrinsic growth rates comparable to the higher end of those reported in the Arctic[43]. The DOMtot additions had a notable lag phase before bacterial growth reached rates ($\mu = 0.35\,d^{-1}$) comparable with the HMW and LMW treatments at 192 h. In the controls, bacterial cell densities doubled once over the 9-day experiment, with low bacterial production (Fig. 2b) and low intrinsic growth rates ($\mu < 0.05\,d^{-1}$), similar to densities and growth rates in natural Arctic bacterioplankton summer communities ($\mu = 0.038–0.08\,d^{-1}$)[43,44].

The degradation of organic matter is influenced by chemical composition, size and reactivity, and the ability of microorganisms to synthesize extracellular enzymes for the hydrolysis of larger compounds[16,45]. Within the spectrum of sea-ice DOM, the greatest

Table 1 | Substrate utilization during experiments of Arctic under-ice surface water enriched with three sea-ice-derived organic matter fractions

Variable/ treatment	Apparent utilization (femtomol C or N bacterial cell^{-1})							Elemental ratio in <600 Da fraction			Number of CUC		
	DOC	dCHO	non-dCHO	DN	DON	NO_3^-	PO_4^{3-}	H/C	C/N	C/S	Total	N	S
Control	–	–	–	–	–	–	–	1.311	50	208	18	4	14
								0.058	*2*	*29*			
DOMtot	38.13	20.7	17.5	4.9	4.22	0.67	0.24	1.374	81	176	136	78	48
	4.9	*2.9*	*4.8*	*0.5*	*0.54*	*0.12*	*0.03*	*0.009*	*12*	*15*			
HMW	18.53	9.8	ns	1.6	0.77*	0.85	0.13	1.298	56	211	87	44	28
	8.41	*2.5*		*0.3*	*0.34*	*0.12*	*0.01*	*0.008*	*5*	*61*			
LMW	22.29	7.3	15.0*	1.9	0.98	0.91	0.17	1.304	55	199	71	41	21
	7.09	*1.9*	*7.6*	*0.2*	*0.21*	*0.11*	*0.01*	*0.009*	*4*	*36*			

Apparent utilization (substrate used per net bacterial cell growth, see Methods) for DOC, dCHO, non-dCHO, DN, DON, NO_3^- and PO_4^{3-} are all significant at $P < 0.001$, except the asterisk denotes $P < 0.05$. –, low growth rates in controls prevented calculation of utilization quota; ns, calculated utilization value not significantly different from zero. Intensity-weighted average elemental H/C, C/N and C/S ratios determined by FT-ICR-MS in the <600 Da molecular fraction and number of Completely Utilized or transformed organic Compounds (CUC), including those containing nitrogen and sulfur, at the end of the 216 h experimental period are also shown. Values represent the mean and, in italics, s.e.m., from triplicate experiments.

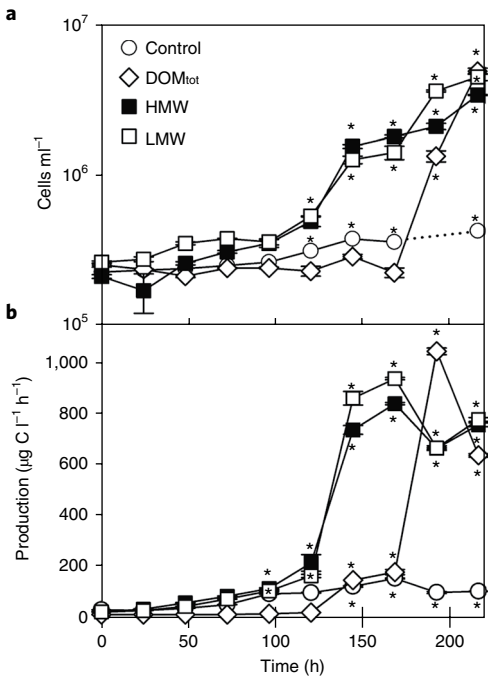

Fig. 2 | Changes in bacterial cell density and productivity over 9 days (216 h) in Arctic under-ice surface water enriched with three sea-ice-derived organic matter fractions (DOM, LMW and HMW). a, Bacterial cell density. **b**, Bacterial production. Mean ± s.e.m., $n = 3$; the asterisk denotes samples significantly different (ANOVA $P < 0.001$ or less) from T_0 values.

proportional utilization was of dCHO in the HMW and LMW treatments containing a high fraction of EPS (originating from ice diatoms[10,31]). This large utilization occurred despite the presence of higher concentrations of other lower molecular weight material (Fig. 1d). Apparent substrate utilization (femtomol carbon or nitrogen per bacterial cell) were lower (that is, more efficient) in the HMW and LMW treatments, and lower for dCHO compared to DOC in each treatment (Table 1) although within the range for marine bacteria[46]. Proportionally more carbohydrate was used to support bacterial growth than other DOM components (Fig. 1c). Arctic bacterioplankton growth rates are positively correlated with DOC (up to saturating concentrations between 200–500 µmol C l^{-1}) and strongly influenced by the concentrations of labile components within the DOM pool[43]. The growth rates measured in this study point to an abundance of labile components in the FYI-derived DOM. Compared to the HMW and LMW treatments, DOMtot enrichment elicited a delayed response as bacteria potentially adjusted to reduced salinity and induction of mechanisms to access the wide pool of DON and sulfur-rich compounds present in the DOMtot fraction. Many small organic compounds seem unavailable to bacteria, forming the unreactive pool of oceanic DOM[15,16,47]. However, we found increased loss or transformation of <600 Da ice-derived nitrogen- and sulfur-rich compounds, in particular in the DOMtot treatment (Table 1). The number of identified molecular formulas <600 Da decreased by 6–11% in all treatments over the incubation period, although no significant changes in average molecular mass was observed (Supplementary Table 2). Between 71 and 136 compounds were completely utilized or transformed (CUC) after 216 h in the additions compared to 18 compounds in the controls (Fig. 3). This suggests that in conditions representative of the stratified meltwater layers in marginal ice zones or under the ice, these small molecules can be utilized by bacterioplankton[48].

The utilization of nitrogen- and sulfur-containing compounds varied, with a comparable utilization of sulfur-containing compounds in the HMW and LMW (Table 1). The average carbon/nitrogen ratio of all detected formulas in the DOMtot addition increased by 17%, while it remained similar in the HMW and LMW treatments. Preferential removal of sulfur-containing compounds increased carbon/sulfur ratios in all treatments (Table 1 and Supplementary Table 1). Although the overall average oxygen/carbon ratio was unchanged in the HMW and LMW treatments, formulas that showed the strongest relative peak magnitude increase in the HMW addition were highly oxidized compounds (higher oxygen/carbon ratio, Fig. 3c), a trend not observed in the LMW fraction (Fig. 3d).

The T_0 bacterioplankton assemblages had a high taxonomic richness (Fig. 4a), with major constituents being Pelagibacteraceae, Rhodobacteraceae, Alteromondales, Oceanospirillales, *Polaribacter* and *Tenacibaculum* (Fig. 4c and Supplementary Fig. 4); a taxonomic profile similar to that of under-ice bacterioplankton in this[49] and other Arctic regions[13,42,50,51]. After 216 h incubation, seawater controls showed minor losses of taxonomic richness, compared with

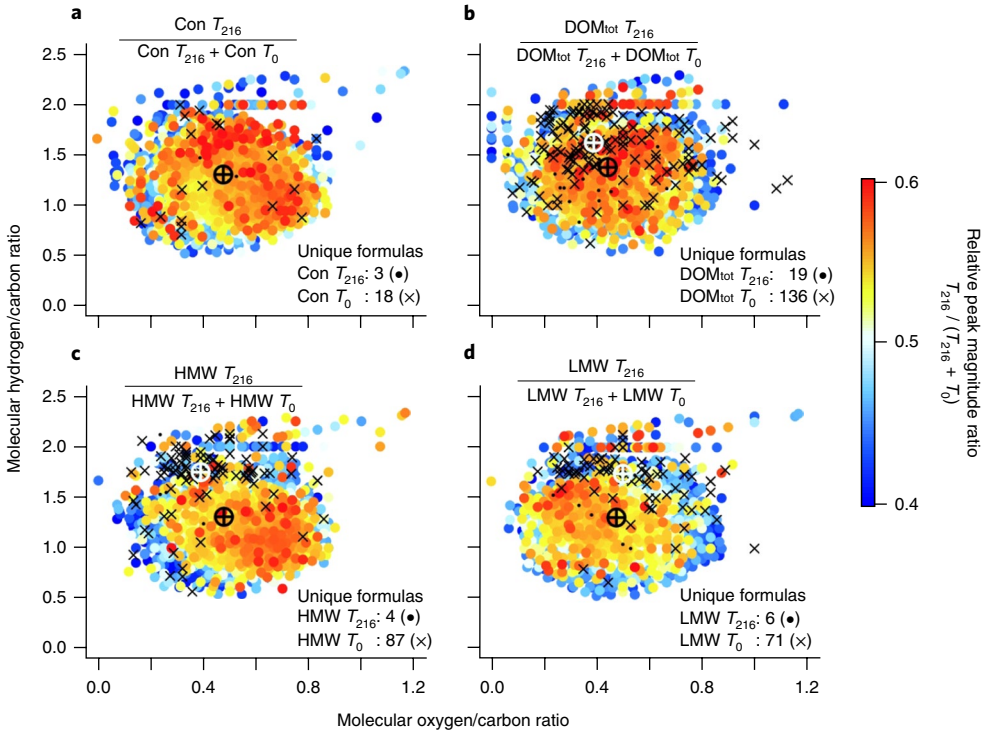

Fig. 3 | Element ratio (van Krevelen) plots of molecular formulas determined by FT-ICR-MS in control and three organic matter enriched treatments over a 216-h incubation. a–d, Control (Con) (**a**), DOMtot (**b**), HMW (**c**) and LMW (**d**) treatments. Each dot represents at least one detected molecular formula represented as the molecular oxygen/carbon and hydrogen/carbon ratio. Colours represent changes in relative peak magnitude ratios over incubation time. Higher values (in red) and the number of unique formulas in controls (crosses) and after 216 days (dots) are indicated. The average elemental compositions for all (black marker) and unique molecular formulas in the control (white marker) are also shown.

major declines in taxonomic richness in the three addition treatments (Fig. 4a; Kruskal–Wallis, $P<0.01$). Dominant bacteria in controls at T_{216} were a single Pelagibacteraceae operational taxonomic unit (OTU; which increased in relative abundance from T_0 to T_{216}), Rhizobiales and Rhodospirillales (*Roseomonas*), *Oxalicibacterium* (3.5% of the T_{216} control assemblages), three *Colwellia*, a *Moritella* and an unidentified Oceanospirillales OTU (Fig. 4c). These OTUs may have been present, but unidentified at T_0 due to lower levels of taxonomic resolution at T_0 compared to T_{216} resolution (the relative abundance of higher taxonomic groupings at T_0 match the relative abundance of lower taxonomic level OTUs within those groupings at T_{216}). Low relative abundance of Rhodobacteraceae OTUs (2.4 % at T_0 and 0.6% overall at T_{216}), and a single Pelagibacteraceae OTU in our samples may reflect the coastal conditions in the Canadian Archipelago. Potential primer bias against these groups has been reported[42,52], although the primers we used amplified these groups[41,53]. In comparison, high abundances of Rhodobacteraceae and SAR11 clades were found in open ocean samples[50]. These changes, together with the measured growth rates and cell densities (Fig. 2a,b), indicate a few major changes in community structure in the controls, apart from a loss of some open water specialists (Rhodobacteraceae) that declined in the microcosms.

DOMtot, HMW and LMW additions resulted in assemblages of significantly lower taxonomic richness. Distinct species assemblage occurred in the DOMtot compared to the HMW and LMW treatments (PERMANOVA, $P<0.01$, Fig. 4b). The former was dominated by OTUs from a subset of mainly Gammaproteobacteria and Bacteriodetes, which accounted for over 94% of all sequences (Fig. 4c and Supplementary Table 3). All OTUs selected for by the DOM additions (with the exception of two Alteromonadales) were also present in the T_{216} control (seawater) bacterial community.

Bacterioplankton assemblages in the HMW and LMW treatments responded similarly (no difference in the NMDS profile, Fig. 4b), with significantly higher relative abundance of Bacteroidetes, Flavobacteriaceae and Gammaproteobacteria. All were taxa found in sea ice and underlying water[49,54], and were able to rapidly utilize the ice-derived DOC and DON. The major Gammaproteobacteria in the enrichments were Alteromonadales, with a number of different enriched *Colwellia* OTUs. *Colwellia* is a successful polar taxon that produces highly adapted extracellular enzymes to break down organic compounds[55]. *Colwellia* live within the sea-ice matrix[54] and also in the underlying water (Fig. 4c), and our results show that representatives of this genus can rapidly and efficiently grow on the sea-ice HMW and LMW fractions. *Colwellia* taxa from the nearshore Chukchi Sea also grow well on riverine DOM[42]. The HMW addition stimulated the growth of Flavobacteriaceae, particularly *Polaribacter* and *Tenacibaculum* (including three OTUs identified at T_0). Bacteriodetes are known degraders of complex organic molecules[56], and *Polaribacter* are facultative or obligate psychrophiles present in seawater and ice[42,49], which are capable of degrading polymeric organic compounds, including phytoplankton and terrestrial DOM[42]. Our results support the observation that *Polaribacter* are sentinel taxa for increased organic matter inputs[42]. *Tenacibaculum* has been isolated from bacterioplankton[41,57] and grows on complex EPS from estuarine diatom biofilms[56].

The DOMtot addition resulted in a different community composition from the HMW and LMW treatments (Fig. 4a–c), stimulating the growth of *Colwellia* taxa (including OTUs that also grew in the HMW and LMW additions), and particularly a number of *Psychrobium*, *Psychromonas* and *Moritella* (Gammaproteobacteria) OTUs (Fig. 4). *Psychromonas* is a psychrophilic genus found across the Arctic[58] that can degrade complex polysaccharides. *Moritella* is

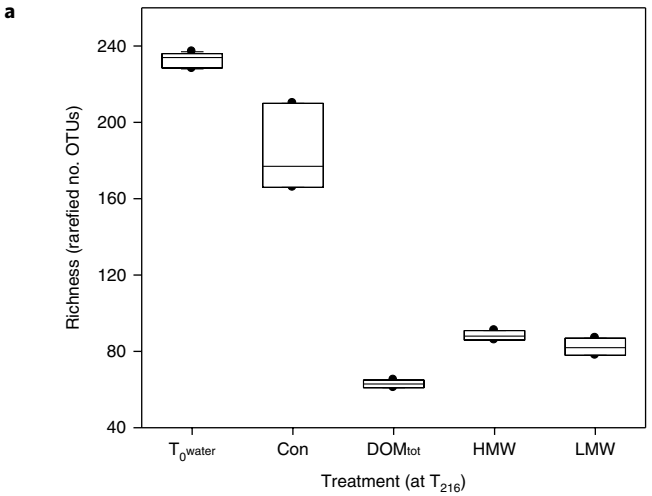

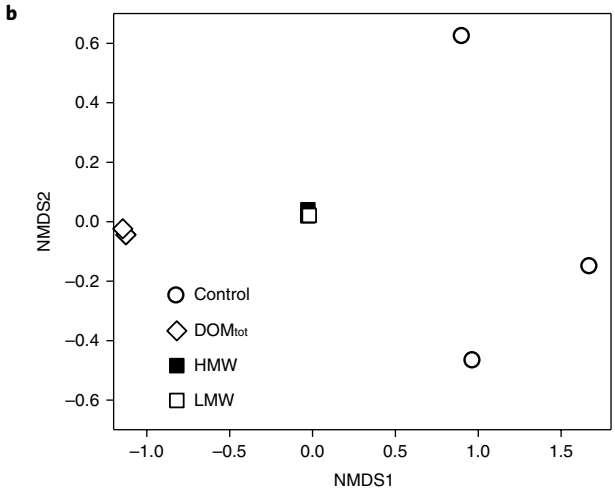

c

Taxon	T_0 water	Control.a	Control.b	Control.c	DOM^{tot}.a	DOM^{tot}.b	DOM^{tot}.c	HWM.a	HWM.b	HWM.c	LMW.a	LMW.b	LMW.c
Acidobacteria													
Acidobacteria_Gp6		1.5	4.1	3.0	0.0	0.0	0.0	0.0	0.0	0.0	0.0	0.0	0.1
Actinobacteria *	1.0												
Cellulomonadaceae; *Cellulomonas*		2.2	3.4	2.5	0.0	0.2	0.1	0.0	0.1	0.1	0.0	0.1	0.1
Bacteroidetes													
Flavobacteriaceae; *Polaribacter*[1]	1.3	0.0	0.0	0.0	0.0	0.0	0.0	0.7	0.3	0.2	0.2	0.5	0.3
Flavobacteriaceae; *Polaribacter*[2]	0.6	0.4	0.1	0.1	0.0	0.1	0.1	2.7	2.8	2.7	2.5	3.8	3.6
Flavobacteriaceae; *Tenacibaculum*[1]	1.0	0.4	0.1	0.0	0.0	0.0	0.0	0.4	0.8	0.6	0.5	0.3	0.5
Flavobacteriaceae; *Tenacibaculum*[2]		0.0	0.1	0.0	0.0	0.0	0.0	0.5	0.7	0.6	0.8	1.0	0.7
Cytophagaceae; *Adhaeribacter*		1.3	1.3	1.9	0.0	0.1	0.2	0.0	0.0	0.1	0.6	0.1	0.1
Firmicutes													
Bacillaceae 1; *Bacillus*		2.8	3.4	8.3	0.6	0.5	1.3	0.9	0.5	0.3	0.3	0.2	0.3
Alphaproteobacteria *	2.5												
Rickettsiales; Pelagibacteraceae	11.3	12.3	23.4	16.7	0.0	0.0	0.0	0.1	0.0	0.0	0.1	0.0	0.0
		1.1	1.9	0.9	0.0	0.0	0.0	0.0	0.0	0.0	0.0	0.0	0.0
Rhizobiales; Hyphomicrobiaceae; *Devosia*	0.1	1.3	7.2	7.6	0.3	0.0	0.3	0.1	0.1	0.0	0.1	0.1	0.1
Rhizobiales; Methylobacteriaceae		3.0	6.5	7.4	0.0	0.1	0.1	0.1	0.0	0.1	0.2	0.1	0.0
Rhodospirillales; *Roseomonas*		2.2	1.5	7.9	0.1	0.1	0.1	0.4	0.0	0.0	0.1	0.0	0.0
Rhodobacterales; Rhodobacteraceae *	2.4	0.0	0.0	0.0	0.0	0.0	0.0	0.0	0.0	0.0	0.0	0.0	0.0
Betaproteobacteria; Burkholderiales *	0.1												
Oxalicibacterium		0.9	0.8	2.8	0.0	0.0	0.0	0.1	0.1	0.0	0.0	0.0	0.1
Gammaproteobacteria; Alteromonadales *	14.9												
denovo15318		0.0	0.0	0.0	0.1	0.1	0.0	0.2	0.3	0.1	0.2	0.3	0.2
Psychorium		0.1	0.2	0.1	3.0	3.0	3.3	1.1	1.0	0.7	2.1	1.7	1.3
Colwellia[1]	0.0	0.0	0.3	0.1	2.5	2.2	2.2	1.5	1.4	1.9	2.2	2.1	2.2
Colwellia[2]		30.5	10.7	9.5	0.4	0.0	0.4	22.4	21.9	18.5	18.9	17.1	22.9
Colwellia[3]		0.8	2.0	0.6	2.7	3.7	3.9	8.2	7.9	6.2	5.3	4.4	8.1
Colwellia[4]	0.0	0.1	0.2	0.0	0.0	0.4	0.0	0.0	0.1	0.0	0.1	0.0	0.0
Colwellia[5]		0.4	2.1	0.2	7.8	7.1	7.8	22.2	28.2	25.0	28.4	22.8	30.5
Thalassomonas	0.0	0.0	0.0	0.0	0.2	0.1	0.2	0.4	0.2	0.2	0.3	0.6	0.2
Moritellaceae; *Moritella*	2.2	2.2	1.6	1.5	63.2	67.1	67.6	27.4	21.4	30.9	26.2	32.4	16.6
Psychromonadaceae; *Psychromonas*	0.1	0.1	0.3	0.1	14.6	10.5	8.3	1.3	1.1	1.5	2.5	3.5	2.6
Gammaproteobacteria; Oceanospirillales *	29.6												
denovo19004	0.0	12.3	3.1	2.4	0.0	0.0	0.0	3.7	3.8	2.9	2.3	2.0	3.2
denovo22973		0.5	0.2	0.3	0.2	0.1	0.1	0.1	0.3	0.3	0.4	0.7	0.4
Oleispira		0.4	0.1	0.1	1.1	1.2	0.7	0.5	0.6	0.7	0.8	0.5	0.5
SUM % of total OTU	67	77	75	74	97	97	97	95	94	94	95	94	94
Total OTU count	*38922*	*2481*	*2523*	*3054*	*4507*	*4735*	*4475*	*3617*	*3554*	*3510*	*3705*	*3863*	*3289*

Fig. 4 | Changes in bacterioplankton taxonomic richness and diversity between under-ice seawater (T_0water) and with addition of three sea-ice-derived organic carbon fractions (DOMtot, HMW, LMW) after 216 h incubation. a, Rarefied taxonomic richness (OTU) of under-ice bacterial assemblages from 16S rRNA OTU at T_0 and T_{216}. **b**, Non-metric multidimensional scaling (NMDS) of taxonomic composition at T_{216}. Note that HMW and LMW data points overlap, permutational multivariate analysis of variance (PERMANOVA), $F_{3,11}=23.43$, $R^2=0.92$, $P=0002$. **c**, Heat map (percentage relative abundance) of bacterial OTU from 454 sequencing of 16S rRNA at T_{216} and in T_0 (from Ion PGM 16S rRNA sequencing) underlying seawater (OTU listed if contributing at least 0.15% of the total sample). Warm colours indicate greater contribution to overall community. OTU sorted by taxonomic groups and species affiliation. The asterisk denotes OTUs identified only to family or higher taxonomic level in T_0 water. SUM% of population, overall contribution of taxa listed to the total OTU count of sample, total OTU sample size given. Mean ± s.e.m., $n=3$ (**a**,**b**), or individual triplicate scores, except T_0 where $n=5$ (**a**) and pooled overall community composition (**c**).

linked to fish disease (as are *Tenacibaculum*) and degrades amino acid-rich mucus and glycoproteins, possibly permitting growth on the DON-rich compounds present and utilized in the DOMtot addition (Fig. 1b and Table 1).

Sea-ice cover in the Arctic Ocean is becoming increasingly seasonal, with an increase in areas of open water and marginal ice zones during the spring–summer months[3,4] and an overall amplification of sea ice–pelagic interactions in extended regions of FYI cover. FYI can support more productive ice-algal communities than MYI[59]. We have shown that different sea-ice DOM fractions are utilized at different rates and stimulate different phylogenetic subsets of the surface-water column bacterioplankton community, with increases in cell density and productivity, and changes in species composition. Our experimental results show that a spectrum of substrates provided by seasonal sea-ice melt, from low to high molecular weight and from nitrogen- to sulfur- rich compounds, are selectively utilized by different taxa within the plankton, resulting in changes in the composition of bacterioplankton. While some taxa of Arctic bacterioplankton are able to use a wide range of substrates, some planktonic taxa within the Alphaproteobacteria and Actinobacteria do not readily use sea-ice DOM. The preferential utilization of sea-ice DOM fractions >10 kDa and >100 kDa by bacterioplankton also has important ramifications for the biogeochemical cycling of organic matter in the Arctic system. These high molecular weight fractions make up the abundant gel-like EPS, which plays a key ecological role such as organic matter aggregation[6] and the production of atmospherically active bioaerosols[26]. Implicit to our results is that these EPS fractions are a highly bioavailable carbon source for under-ice microbial communities.

Unravelling the significance and repercussions of our results for the Arctic Ocean requires consideration of various factors involved in the cycling of DOM. During our experiment, grazing, DOM production by autotrophic cells and photodegradation were controlled for, allowing the identification of bacterial responses to sea-ice DOM fractions without potential changes in DOM concentrations or composition due to these other factors. Viral activity, responses to inorganic nutrients and low salinity conditions (DOMtot treatment) may have affected net changes in bacterial assemblages over time and between treatments[60]. Photochemical degradation of DOM under the ice is considered negligible[61], although it is probable that photodegradation will increase with increased melt pond coverage and associated light transmission through the ice cover[11], which can also lead to increased under-ice phytoplankton blooms[11,62].

By showing that FYI DOM fractions are used efficiently by subgroups of surface-water bacterial communities, our results indicate that the continued shift towards a seasonal sea-ice regime in the Arctic Ocean, while having only a minor impact on Arctic Ocean DOM inventories, may have a disproportionate impact on DOM remineralisation in surface waters. This dual understanding of DOM cycling in the seasonally ice-covered Arctic reconciles divergent perspectives on inventories[63] and rates[6,11], both fundamental to constrain ocean-climate models.

Climate change has resulted in FYI already becoming the dominant type of ice in the Arctic Ocean[3,4], with a complete seasonal ice cover predicted to occur over coming decades[12]. More labile DOM will be released from sea ice to the ocean surface under future sea-ice cover scenarios in an Arctic Ocean that will remain ice dominated[30,59]. How large areas previously covered by MYI will respond to changes in sea-ice biochemistry and seasonal dynamics remains a fundamental question in defining the role of the 'new' Arctic in biogeochemical cycles. Earth system models incorporating the role of DOM across the Arctic[64] require a mechanistic understanding of the composition and turnover of DOM to constrain biogeochemical fluxes within the ice and at the ice–water interface under future climate scenarios. We propose that DOM fractions produced by sea ice, once released into surface waters, provide ecological niches for taxon-specific bacterial activity. Based on our results, the expansion of FYI and altered temporal and spatial gradients in the release of sea-ice-derived DOM fractions will increase bacterial respiration and modify microbial community structure and dynamics at sea ice–water interfaces, including ice margins. We further propose that these changes will affect the cycling of key elements, and possibly microbial evolutionary pathways, in the warming Arctic Ocean.

Online content

Any methods, additional references, Nature Research reporting summaries, source data, statements of data availability and associated accession codes are available at https://doi.org/10.1038/s41558-018-0391-7.

Received: 8 October 2017; Accepted: 13 December 2018;
Published online: 21 January 2019

References

1. Cohen, J. et al. Recent Arctic amplification and extreme mid-latitude weather. *Nat. Geosci.* **7**, 627–637 (2014).
2. Stroeve, J. C., Markus, T., Boisvert, L., Miller, J. & Barrett, A. Changes in Arctic melt season and implications for sea ice loss. *Geophys. Res. Lett.* **41**, 1216–1225 (2014).
3. Swart, N. C., Fyfe, J. C., Hawkins, E., Kay, J. E. & Jahn, A. Influence of internal variability on Arctic sea-ice trends. *Nat. Clim. Change* **5**, 86–89 (2015).
4. Perovich, D. K. et al. *Arctic Report Card 2015* (NOAA, 2015); https://www.arctic.noaa.gov/Report-Card/Report-Card-2015/ArtMID/5037/ArticleID/217/Sea-Ice
5. Clark, G. F. et al. Light driven tipping points in polar ecosystems. *Glob. Change Biol.* **19**, 3749–3761 (2013).
6. Vancoppenolle, M. et al. Role of sea ice in global biogeochemical cycles: emerging views and challenges. *Quat. Sci. Rev.* **79**, 207–230 (2013).
7. Krembs, C. & Deming, J. W. in *Psychrophiles: from Biodiversity to Biotechnology* (eds Margesin, R. et al.) 247–264 (Springer, Berlin, 2008).
8. Krembs, C., Eicken, H. & Deming, J. W. Exopolymer alteration of physical properties of sea ice and implications for ice habitability and biogeochemistry in a warmer Arctic. *Proc. Natl Acad. Sci. USA* **108**, 3653–3658 (2011).
9. Underwood, G. J. C. et al. Broad-scale predictability of carbohydrates and exopolymers in Antarctic and Arctic sea ice. *Proc. Natl Acad. Sci. USA* **110**, 15734–15739 (2013).
10. Aslam, S. N., Michel, C., Niemi, A. & Underwood, G. J. C. Patterns and drivers of carbohydrate budgets in ice algal assemblages from first year Arctic sea ice. *Limnol. Oceanogr.* **61**, 919–937 (2016).
11. Leu, E. et al. Arctic spring awakening – steering principles behind the phenology of vernal ice algal blooms. *Prog. Oceanogr.* **139**, 151–170 (2015).
12. Arctic Monitoring and Assessment Programme *Snow, Water, Ice and Permafrost* Summary for Policy-Makers (AMAP , Oslo, 2017).
13. Bowman, J. S. et al. Microbial community structure of Arctic multiyear sea ice and surface seawater by 454 sequencing of the 16S RNA gene. *ISME. J.* **6**, 11–20 (2012).
14. Hatam, I., Lange, B., Beckers, J., Haas, C. & Lanoil, B. Bacterial communities from Arctic seasonal sea ice are more compositionally variable than those from multi-year sea ice. *ISME J.* **10**, 2543–2552 (2016).
15. Verdugo, P. Marine microgels. *Ann. Rev. Mar. Sci.* **4**, 375–400 (2012).
16. Benner, R. & Amon, R. M. W. The size-reactivity continuum of major bioelements in the ocean. *Annu. Rev. Mar. Sci.* **7**, 185–205 (2015).
17. Amon, R. M. W., Fitznar, H. P. & Benner, R. Linkages among the bioreactivity, chemical composition, and diagenetic state of marine dissolved organic matter. *Limnol. Oceanogr.* **46**, 287–297 (2001).
18. Riedel, A., Michel, C. & Gosselin, M. Seasonal study of sea-ice exopolymeric substances on the Mackenzie shelf: implications for transport of sea-ice bacteria and algae. *Aquat. Microb. Ecol.* **45**, 195–206 (2006).
19. Juhl, A. R., Krembs, C. & Meiners, K. M. Seasonal development and differential retention of ice algae and other organic fractions in first-year Arctic sea ice. *Mar. Ecol. Prog. Ser.* **436**, 1–16 (2011).
20. Smith, R. E. H., Gosselin, M., Kudoh, S., Robineau, B. & Taguchie, S. DOC and its relationship to algae in bottom ice communities. *J. Mar. Syst.* **11**, 71–80 (1997).
21. Michel, C., Riedel, A. & Mundy, C. J. *Biological Investigation of First-Year Sea Ice Near Resolute Bay, Nunavut, Spring to Early Summer 2001*. Canadian Data Report of Hydrography and Ocean Sciences 160 (Government of Canada, 2003).
22. Riedel, A., Michel, C. & Gosselin, M. Grazing of large-sized bacteria by sea-ice heterotrophic protists onthe Mackenzie shelf during the winter–spring transition. *Aquat. Microbiol. Ecol.* **50**, 25–38 (2017).

23. Meiners, K., Brinkmeyer, R., Granskog, M. A. & Lindfors, A. Abundance, size distribution and bacterial colonization of exopolymer particles in Antarctic sea ice (Bellingshausen Sea). *Aquat. Microb. Ecol.* **35**, 283–296 (2004).
24. Niemi, A., Meisterhans, G. & Michel, C. Response of under-ice prokaryotes to experimental sea-ice DOM enrichment. *Aquat. Microb. Ecol.* **73**, 17–28 (2014).
25. Assmy, P. et al. Floating ice-algal aggregates below melting Arctic sea ice. *PLoS ONE* **8**, e76599 (2013).
26. Wilson, T. W. et al. A marine biogenic source of atmospheric ice-nucleating particles. *Nature* **525**, 234–238 (2015).
27. Holding, J. M. et al. Autochthonous and allochthonous contributions of organic carbon to microbial food webs in Svalbard fjords. *Limnol. Oceanogr.* **62**, 1307–1323 (2017).
28. Jørgensen, L., Stedmon, C. A., Kaartokallio, H., Middelboe, M. & Thomas, D. N. Changes in the composition and bioavailability of dissolved organic matter during sea ice formation. *Limnol. Oceanogr.* **60**, 817–830 (2015).
29. Galindo, V. Biological and physical processes influencing sea ice, under-ice algae, and dimethylsulfoniopropionate during spring in the Canadian Arctic Archipelago. *J. Geophys. Res. Oceans* **119**, 3746–3766 (2014).
30. Meiners, K. M. & Michel, C. in *Sea Ice* 3rd edn (ed. Thomas, D. N.) 415–432 (Wiley Blackwell, Oxford, 2017).
31. Aslam, S. N., Strauss, J., Thomas, D. N., Mock, T. & Underwood, G. J. C. Identifying metabolic pathways for production of extracellular polymeric substances (EPS) by the diatom *Fragilariopsis cylindrus* inhabiting sea ice. *ISME J.* **12**, 1237–1251 (2018).
32. Sleighter, R. L. & Hatcher, P. G. The application of electrospray ionization coupled to ultrahigh resolution mass spectrometry for the molecular characterization of natural organic matter. *J. Mass Spectrom.* **42**, 559–574 (2007).
33. Shen, Y., Fichot, C. G. & Benner, R. Dissolved organic matter composition and bioavailability reflect ecosystem productivity in the Western Arctic Ocean. *Biogeosciences* **9**, 4993–5005 (2012).
34. Michel, C., Ingram, R. G. & Harris, L. R. Variability in oceanographic and ecological processes in the Canadian Arctic Archipelago. *Prog. Oceanogr.* **71**, 379–401 (2006).
35. Niemi, A., Michel, C., Hille, K. & Poulin, M. Protist assemblages in winter sea ice: setting the stage for the spring ice algal bloom. *Polar Biol.* **34**, 1803–1817 (2011).
36. Chin, W., Orellana, M. V. & Verdugo, P. Spontaneous assembly of marine dissolved organic matter into polymer gels. *Nature* **391**, 568–572 (1998).
37. Mundy, C. J. et al. Role of environmental factors on phytoplankton bloom initiation under landfast sea ice in Resolute Passage, Canada. *Mar. Ecol. Prog. Ser.* **497**, 38–49 (2014).
38. Elliott, A. et al. Spring production of mycosporine-like amino acids and other UV-absorbing compounds in sea ice-associated algae communities in the Canadian Arctic. *Mar. Ecol. Prog. Ser.* **541**, 91–104 (2015).
39. Arnosti, C. & Steen, A. Patterns of extracellular enzyme activities and microbial metabolism in an Arctic fjord of Svalbard and in the northern Gulf of Mexico: contrasts in carbon processing by pelagic microbial communities. *Front. Microbiol.* **4**, 1 (2013).
40. Steen, A. D. & Arnosti, C. Picky, hungry eaters in the cold: persistent substrate selectivity among polar pelagic microbial communities. *Front. Microbiol.* **5**, 527 (2014).
41. Teeling, H. et al. Recurring patterns in bacterioplankton dynamics during coastal spring algae blooms. *eLife* **5**, e11888 (2016).
42. Sipler, R. E. et al. Microbial community response to terrestrially derived dissolved organic matter in the coastal Arctic. *Front. Microbiol.* **8**, 1018 (2017).
43. Ortega-Retuerta, E. et al. Carbon fluxes in the Canadian Arctic: patterns and drivers of bacterial abundance, production and respiration on the Beaufort Sea margin. *Biogeosciences* **9**, 3679–3692 (2012).
44. Kirchman, D. L. et al. Standing stocks, production, and respiration of phytoplankton and heterotrophic bacteria in the western Arctic Ocean. *Deep Sea Res. Part 2 Top. Stud. Oceanogr.* **56**, 1237–1248 (2009).
45. Arnosti, C. Microbial extracellular enzymes in the marine carbon cycle. *Annu. Rev. Mar. Sci.* **3**, 401–425 (2011).
46. Troussellier, M., Bouvy, M., Courties, C. & Dupuy, C. Variation of carbon content among bacterial species under starvation conditions. *Aquat. Microb. Ecol.* **13**, 113–119 (1997).
47. Hansell, D. A. & Carlson, C. A. Dissolved organic matter in the ocean: a controversy stimulates new insights. *Oceanography* **22**, 202–211 (2009).
48. Ksionzek, K. B. et al. Dissolved organic sulfur in the ocean: biogeochemistry of a petagram inventory. *Science* **354**, 456–459 (2016).
49. Yergeau, E. et al. Metagenomic survey of the taxonomic and functional microbial communities of seawater and sea ice from the Canadian Arctic. *Sci. Rep.* **7**, 42242 (2017).
50. Zeng, Y. et al. Phylogenetic diversity of planktonic bacteria in the Chukchi Borderland region in summer. *Acta Oceanologica Sininica* **32**, 66–74 (2013).
51. Pedrós-Alió, C., Potvin, M. & Lovejoy, C. Diversity of planktonic microorganisms in the Arctic Ocean. *Prog. Oceanogr.* **139**, 233–243 (2015).
52. Parada, A. E., Needham, D. M. & Fuhrman, J. A. Every base matters: assessing small subunit rRNA primers for marine microbiomes with mock communities, time series and global field samples. *Environ. Microbiol.* **18**, 1403–1414 (2015).
53. Herlemann, D. P. R. et al. Transitions in bacterial communities along the 2000 km salinity gradient of the Baltic Sea. *ISME J.* **5**, 1571–1579 (2011).
54. Deming, J. W. & Collins, R. E. in *Sea Ice* 3rd edn (ed. Thomas, D. N.) 326–351 (Wiley, Oxford, 2017).
55. Methé, B. A. et al. The psychrophilic lifestyle as revealed by the genome sequence of *Colwellia psychrerythraea* 34H through genomic and proteomic analyses. *Proc. Natl Acad. Sci. USA* **102**, 10913–10918 (2005).
56. Bohórquez, J. et al. Different types of diatom-derived extracellular polymeric substances drive changes in heterotrophic bacterial communities from intertidal sediments. *Front. Microbiol.* **8**, 245 (2017).
57. Frette, L., Jørgensen, N. O., Irming, H. & Kroer, N. *Tenacibaculum skagerrakense* sp. nov., a marine bacterium isolated from the pelagic zone in Skagerrak, Denmark. *Int. J. Syst. Evol. Microbiol.* **54**, 519–524 (2004).
58. Groudieva, T., Grote, R. & Antranikian, G. *Psychromonas arctica* sp. nov., a novel psychrotolerant, biofilm-forming bacterium isolated from Spitzbergen. *Int. J. Syst. Evol. Microbiol.* **53**, 539–545 (2003).
59. Lange, B. A. et al. Comparing springtime ice-algal chlorophyll a and physical properties of multi-year and first-year sea ice from the Lincoln Sea. *PLoS ONE* **10**, e0122418 (2015).
60. Thingstad, T. F., Våge, S., Storesund, J. E., Sandaa, R.-A. & Giske, J. A theoretical analysis of how strain-specific viruses can control microbial species diversity. *Proc. Natl Acad. Sci. USA* **111**, 7813–7818 (2014).
61. Logvinova, C. L., Frey, K. E., Mann, P. J., Stubbins, A. & Spencer, R. G. M. Assessing the potential impacts of declining Arctic sea ice cover on the photochemical degradation of dissolved organic matter in the Chukchi and Beaufort Seas. *J. Geophys. Res. Biogeosci.* **120**, 2326–2344 (2015).
62. Horvat, C. et al. The frequency and extent of sub-ice phytoplankton blooms in the Arctic Ocean. *Sci. Adv.* **3**, e1601191 (2017).
63. Anderson, L. G., & Amon, R. M. W. in *Biogeochemistry of Marine Dissolved Organic Matter* 2nd edn (eds Hansell, D. A. & Carlson, C. A.) 609–633 (Academic Press, Boston, 2015).
64. Elliot, S. et al. Strategies for the simulation of sea ice organic chemistry: Arctic tests and development. *Geosciences* **7**, 52 (2017).

Acknowledgements

G.J.C.U. was funded by grants no. NE/D00681/1 and no. NE/E016251/1 from the UK Natural Environment Research Council. C.M. received financial support from the Natural Sciences and Engineering Council of Canada (Individual Discovery Grant), the International Governance Strategy (Fisheries and Oceans Canada) and the Polar Continental Shelf Program (Natural Resources Canada) for the project Sea Ice BIOTA (Biological Impacts of Trends in the Arctic). G.M. received a Visiting Fellowship in Canadian Government Laboratory from the Natural Sciences and Engineering Council of Canada. C. Burau is acknowledged for performing solid-phase extraction. We thank S. Duerksen, D. Jordan, M. Poulin and A. Reppchen for their help in the field and laboratory. We also appreciate support from the Resolute Bay Hunters and Trappers Association and the logistical support from the Polar Continental Shelf Program in Resolute, Nunavut.

Author contributions

G.J.C.U., C.M. and A.N. designed the study. G.J.C.U., C.M. and G.M. conducted the experiments. M.W. carried out FT-ICR-MS analysis. G.J.C.U., C.M., C.B., G.M., A.N., B.P.K. and A.J.D. analysed the data. G.J.C.U., C.M., B.P.K. and A.J.D. wrote the manuscript.

Competing interests

The authors declare no competing interests.

Additional information

Supplementary information is available for this paper at https://doi.org/10.1038/s41558-018-0391-7.

Reprints and permissions information is available at www.nature.com/reprints.

Correspondence and requests for materials should be addressed to G.J.C.U.

Journal peer review information: Nature Climate Change thanks David Kirchman and other anonymous reviewer(s) for their contribution to the peer review of this work.

Publisher's note: Springer Nature remains neutral with regard to jurisdictional claims in published maps and institutional affiliations.

Methods

Surface water and FYI sea-ice cores were collected on 1 May 2012 at a first-year sea-ice station (74.75° N, 95.50° W) located about 2 km offshore in Resolute Passage, Canadian Arctic Archipelago (Nunavut). Resolute Passage is typically covered by landfast FYI from late November to the beginning of July. Twenty-six (26) sea-ice cores were collected using a manual ice corer (Mark II coring system, 9-cm internal diameter, Kovacs Enterprises). The bottom 3-cm sections of the cores, where most of the sea-ice biomass is found[29], were cut with a clean stainless steel saw and stored in sterile Whirl-Pak bags. Surface water (60 l) was collected using a pump installed on an under-ice arm, reaching out 1 m from the hole. The water collected from the ice interface was free of ice (initial flow with potential presence of ice was left out). The acid-washed Nalgene container in which the water was transferred was rinsed three times with the sample before filling. The sea ice and surface water samples were transported back to the shore laboratory where they were kept in the dark at 0 °C until the beginning of the experiments. Experiments began the day after sample collection to allow the ice samples to melt slowly overnight. Experiments and sample processing were conducted at the Polar Continental Shelf Program laboratory facilities, Resolute Bay, Nunavut.

Starting conditions. Sea-ice core sections were melted within 24 h of collection in sterile Whirl-Pak bags at 4 °C in darkness without the addition of filtered seawater. Melted material was filtered through pre-combusted (450 °C for 24 h) Whatmann GF/F and pooled, giving a total volume of 3,225 ml, and stored at 4 °C.

Four fully replicated treatments were established, with 30 sterile Whirl-Pak bags each filled with 300 ml of starting condition media for each of the four treatments. Control treatments consisted of under-ice seawater filtered through a 3 -µm filter to remove larger protists and grazers. DOMtot enrichments consisted of GF/F filtered DOM obtained from melted bottom-ice core sections, added to filtered (3-µm filter) under-ice seawater (DOM/seawater ratio was 1/5.3), giving a final DOC concentration of 451 µmol C l^{-1} (Supplementary Table 1). Two molecular weight-fractionated DOM enrichments (a HMW-enhanced DOM fraction retained above an 100 kDa filter, known to be rich in diatom EPS larger than 100 kDa, and an intermediate LMW EPS-rich DOM fraction retained between 10 kDa and 100 kDa filters) were established by sequentially filtering 1,715 ml of the melted ice core DOM extract through 100 kDa and 10 kDa molecular filters (Amicon Millipore) to separate the polydisperse DOM pool into two molecular weight fractions. The filter sizes correspond to those used to investigate transparent exopolymer particle (TEP) formation in seawater[65], and in studies of diatom and algal EPS investigations, with the 10–100 kDa providing a separation between the lower and higher molecular weight colloidal exudates produced by polar algae[16,66,67].

The HMW fraction contained the dissolved organic constituents retained in a final volume of 195 ml above a 100 kDa molecular filter (from 1,715 ml filtrate). This 100 kDa-enriched fraction was added to 9.3 l of (3-µm filtered) under-ice seawater to give a final DOC concentration of 304 µmol C l^{-1} (Table 1). The 1,520 ml of 100 kDa filtrate was reduced to a final volume of 215 ml above a 10 kDa Amicon filter, and this fraction (LMW, <100 kDa and >10 kDa molecular weight) was added to 9.3-l filtered under-ice seawater to give a final DOC concentration of 562 µmol C l^{-1} (Table 1). The Whirl-Pak bags were sealed and placed in a chilled incubator facility, and maintained in darkness at an average temperature of −1.72 °C ± 0.021 °C (Hobo data loggers) over a period of 216 h. Bags were checked and rotated daily. Every 24 h, three replicate bags from each treatment and controls were sampled. Each bag was manually mixed and subsamples were collected and analysed at each experimental time for prokaryotic abundance and production, DOC, dissolved nitrogen (DN), inorganic nutrients (phosphate, PO_4^{3-}; silicic acid, $SiOH_4$; nitrate, NO_3^- and nitrite, NO_2^-), and carbohydrate concentrations.

Analytical water chemistry. Surface water and sea-ice salinity was measured with a salinometer probe (Portsal 8410A, Technel). A 13-ml sample was taken for nutrient analysis. Filtered samples (pre-combusted Whatman GF/F filters) were stored at −80 °C for later determination of NO_3^-, NO_2^-, PO_4^{3-} and $Si(OH)_4$ concentrations using a SmartChem discrete analyser (Westco Scientific Instruments). Nutrient chemistries were adapted from[68].

Then 25 ml water was filtered through pre-combusted (450 °C for 5 h) GF/F filters, with the first 5 ml discarded as a rinse and 20 ml stored in pre-combusted acid-washed amber bottles at 4 °C in a fridge after being acidified with 50% H_3PO_4. DOC and DN were measured on a Shimadzu TOC-VCPH analyser with an ASI-V auto sampler and TNM-1 Total Nitrogen module, using high-temperature catalytic combustion[69]. The analyses were systematically checked against consensus reference material (that is, deep seawater reference) from the Hansell's Certified Reference Materials program. The remaining 250 ml was GF/F filtered into acid-washed plastic bottles and frozen at −20 °C for subsequent carbohydrate, EPS and FT-ICR-MS analysis.

Dissolved carbohydrate. Filtrates were used for dCHO and a subsample (0.4 ml) of GF/F filtrate was used to determine total dissolved carbohydrate concentration ($dCHO_{TOTAL}$) using a modified phenol sulfuric acid assay[70] as described by ref. [10]. The modified Dubois assay measures a range of neutral sugars (hexoses and pentoses), as well as acidic carbohydrates (uronic acids)[70]. It shows different sensitivities to different constituents, but is a stable assay and widely used in microbial ecology studies of EPS and microbial polysaccharides[8,10,66,71,72]. To estimate EPS concentrations, a 3-ml subsample of GF/F filtrate was subject to a 70% v/v ethanol precipitation for 24 h at 4 °C, followed by centrifugation to isolate the EPS pellet. The precipitation of EPS using an alcohol solvent is an established polysaccharide chemistry technique[71,73]. The pellet was resuspended in distilled water and analysed using the phenol sulfuric acid assay[10]. Glucose was used as a standard, with standard curves modified with sodium chloride where necessary to correspond to the salinity of the fraction being measured. Carbohydrate concentrations were calculated as glucose-carbon-equivalents and converted to µmol C l^{-1}.

Ultrahigh resolution mass spectrometry (FT-ICR-MS) and data evaluation. Before FT-ICR-MS analysis, 100-ml aliquots of each sample were desalted (dialysis at 8 kDa, 24 h in 1 l) and lyophilized. Since remnants of salt prevented electrospray ionization, the dried samples were redissolved in 15 ml ultrapure water (ultrasonification for 15 min). Then 10 ml aliquots of the redissolved sample were acidified to pH2 (ultrapure HCl, Merck) and solid-phase extracted (PPL adsorber, 200-mg cartridge, Agilent[74]). FT-ICR-MS analyses were carried out as described previously[75]. Before analysis, DOM extracts were diluted with methanol/water (1/1, v/v). Samples were ionized by electrospray ionization (ESI, Apollo II electrospray ionization source, Bruker Daltonik) in negative mode at an infusion flow rate of 120 µl h^{-1} on a FT-ICR-MS (SolariX, Bruker Daltonik) equipped with a 12 T refrigerated actively shielded superconducting magnet (Bruker Biospin). Three hundred scans were added to one mass spectrum. The magnitude threshold for the peak detection was set to a signal/noise ratio of ≥4. Mass spectra were recalibrated internally with compounds, which were repeatedly identified in marine DOM samples[69] (*m/z*: 247.06120, 297.13436, 327.14493, 369.15549, 397.15041, 439.16097, 483.18719, 551.24979, 595.23962). The average mass error of the detected compounds was below 50 ppb.

All ions were individually charged as confirmed by the spacing of the related $^{12}C_n$ and $^{13}C_1C_{n-1}$ mass peaks. The spectra were evaluated in the mass range of 200–600 *m/z*. The base peak in this mass range was defined as 100%, and relative intensities for all other peaks were calculated accordingly. For the process of formula assignment only peaks with a relative intensity between 1% and 100% were considered. Molecular formulas were calculated from *m/z* values allowing for elemental combinations $^{12}C_{0-\infty}{}^{13}C_{0-1}{}^{1}H_{0-\infty}{}^{14}N_{0-3}{}^{16}O_{0-\infty}{}^{32}S_{0-2}{}^{34}S_{0-1}$ and a mass accuracy threshold of $|\Delta m| \leq 0.2$ ppm. The double bond equivalent (DBE = 1 + ½(2C − H + N)) of a valid neutral formula had to be an integer value ≥0 and ≤20 and the nitrogen-rule was applied. Combinations of N_2S_2 ($n = 614$) and N_3S_2 ($n = 19$) were excluded because of a higher average mass error compared to all other elemental combinations. Formulas that were detected in a process blank (PPL extraction of ultrapure water) or in the list of potential surfactants[76], as well as formulas containing a ^{13}C or ^{34}S isotope and those that did not correspond to a parent formula (^{12}C, ^{32}S) were also removed from the dataset. The final dataset contained 95,434 identified molecular formulas. Intensity-weighted average molecular masses and element ratios were calculated based on normalized peak magnitudes. It should be noted that the elemental ratios determined by FT-ICR-MS differ from bulk ratios due to differences in compound specific ionization efficiencies in electrospray ionization. For comparison of treatments, the average peak magnitude for each molecular formula within a treatment was calculated ($n = 3$). The evaluation of unique molecular formulas using van Krevelen diagrams was performed only for those formulas that occurred in either all or none of the three samples of a treatment.

Bacterial abundance and productivity. The abundance of bacteria was determined by flow cytometry. Duplicate 4-ml subsamples were fixed with glutaraldehyde Grade I (0.5% final concentration; Sigma) in the dark at 4 °C for 30 min, and then frozen at −80 °C until analysis. Bacteria samples were stained with SYBR Green I (Invitrogen) and counted with an Epics Altra flow cytometer (Beckman Coulter) fitted with a 488-nm laser operated at 18 mW[24]. The green fluorescence of nucleic acid-bound SYBR Green I was measured at 525 +/− 5 nm. Cytograms obtained were analysed using Expo32 v1.2b software (Beckman Coulter). The addition of DOM increased the background fluorescence of the samples due to non-specific binding of SYBR Green I to DOM and EPS. Bacteria could not be differentiated from this added fluorescence using the standard approach where bacterial populations are identified on a side scatter versus green fluorescence scatterplot[77,78]. Because of the shift in emission wavelengths on binding of SYBR Green I to DNA[79], it was possible to discriminate bacteria from background fluorescence. On a scatterplot of green versus red fluorescence (measured at 610 nm/BP 20 nm), bacteria stained with SYBR Green I fell on a narrow diagonal, while DOM and EPS had a higher red fluorescence for a given green fluorescence intensity. Using this approach, bacterial abundance was practically identical in all treatments at T_0 (see Fig. 2a), when the influence of added DOM and TEP was largest.

Bacterial production was measured from the incorporation rates of the tritiated (^3H) amino acid leucine, according to ref. [80]. This method measures protein production in both bacteria and archaea[81], therein referred to as bacterioplankton. Triplicate 1.2-ml subsamples and two controls were inoculated with ^3H-leucine (specific activity: 60 Ci $mmol^{-1}$; final concentration 10 nM). The controls were immediately spiked with 50% trichloroacetic acid (TCA, 5% final concentration).

All five vials (measurement and controls) were incubated in the dark at 4 °C for 4 h. At the end of the incubation, TCA (5% final concentration) was added to the vials and samples were frozen at −80 °C until final analysis in our main laboratory. Analyses were performed within 2 months of sample collection. The thawed samples were centrifuged at 14,000 r.p.m. for 10 min. The supernatant was removed and pellets were rinsed with 1 ml of TCA (5% final concentration). The TCA was removed after two more rounds of centrifugation. Scintillation cocktail (Ecolume, MP Biomedicals) was added to the vials, and bacterial cells were resuspended by vortex mixing. ^{3}H-leucine incorporation was measured using a liquid scintillation counter (TRI-CARB 2100 TR, Packard Bio-Science) after 48 h of incubation in the dark at 4 °C.

Cell-normalized apparent substrate utilization quotas (as femtomol carbon or nitrogen per cell) were calculated from linear regressions between the declining concentrations of substrate and increasing bacterial cell numbers (Table 1) in the three addition treatments. Because there was no significant growth in the controls, no significant regressions could be derived.

Bacterioplankton community analysis. The composition of the bacterial community at the beginning of the experiment (T_0) was determined by ref. [82] on the identical water samples used to set up this experiment. Partial 16S ribosomal (rRNA) gene amplicons were generated using the universal primers F343 (5'-TACGGRAGGCAGCAG-3') and R534 (5-ATTACCGCGGCTGCTGGC-3'). Sequencing was performed on an Ion Torrent PGM using the Ion 314 chip and the Ion PGM Sequencing 200 kitV2 (Life Technologies) following the manufacturer's instructions. For full details, see[82].

The composition of the bacterial community at the end of the experiment was assessed from a 250-ml sample, from a parallel set of identical treatment bags ($n=3$), which was filtered through sterile 0.22-µm Millipore Durapore filters and frozen at −80 °C immediately after filtering, following the methods in ref. [56]. DNA was extracted from the frozen filters using the MoBio PowerSoil DNA isolation kit using the manufacturer's protocol. 16S rRNA gene libraries were constructed from these DNA extracts. The sequences of the primers specific to bacterial 16S rRNA genes were: Bakt_341F (5′-CCTACGGGNGGCWGCAG-3′ and Bakt_805R (5′-ACHVGGGTATCTAATCC-3′)[49]. GS FLX Titanium adaptors were at the 5′-end of the Bakt primers: adaptor A for the forward primer (5'-CGTATCGCCTCCCTCGCGCCATCAG-3′) and B for the reverse primer (5'-CTATGCGCCTTGCCAGCCCGCTCAG-3′). Sample-specific 10-basepair (bp) barcodes were located between the B adaptor and Bakt_805R.

Analysis of pyrosequence data. Sequences were analysed using the QIIME (Quantitative Insights Into Microbial Ecology) pipeline and associated modules[83]. Pyrosequencing data were fully denoised using AmpliconNoise[84]. Sequences were removed if they had errors in the 10-bp barcodes and taxon-specific primers, were <450 bp long, had low quality scores (<25) and ≥7 bp homopolymer inserts. Pyrosequences were clustered into OTUs at the 95% similarity level using USearch, and the associated de novo chimera checker[85] was used to detect and remove chimeras and OTUs represented by fewer than four sequences across all samples. Representative sequences from each OTU were assigned to a taxonomic group using the Ribosomal Database Project classifier algorithm[86] version 9, and using a 95% similarity cut off. Eighty per cent of raw pyrosequencing passed our quality filtering and denoising, providing 43,697 sequences from 661 different OTUs. Sequence data are available at the European Bioinformatics Institute, http://www.ebi.ac.uk, under accession number PRJEB20754 (fastq file names correspond to sample identities).

To compare the T_0 and T_{216} data, OTUs captured from T_{216} (as described above) were used as a custom database against which T_0 OTUs were picked using VSEARCH[87]. T_0 data were already denoised and quality filtered (see ref. [82]) but checks for chimeric sequences were included in the new analysis, although none were detected. This approach provides an ideal solution to combine the two datasets from different sequencing technologies because the resultant amplicon are directly compared and, in this case, start within 2 bp of each other on the forward primers, thus covering the same region of the 16S rRNA gene. Sequences classified as unidentified bacteria were maintained across datasets, but cyanobacterial plastid sequences were removed because we were focusing on the heterotrophic bacteria. Amplicon data were normalized via rarefaction before comparing alpha (taxonomic richness) and beta (NMDS analysis based on Bray–Curtis distances) diversity measurements between samples.

Statistical analysis. Differences over a time period and between treatments were tested using one-way and two-way ANOVA with Tukey post hoc tests, using Minitab v.13.3 (Minitab). Data were tested for normality and homogeneity of variances and log transformation was performed on data deviating from these assumptions. Comparison of changes in taxonomic composition were conducted using ANOVA, adjusting P values to accommodate multiple testing. The molecular similarity between treatments (FT-ICR data) was assessed by applying cluster analyses based on untransformed normalized peak magnitudes and Bray–Curtis similarity[88] and software R and Primer, version 6. All statistical differences mentioned in the paper are significant at $P<0.05$ or less.

Data availability

Experimental https://doi.org/10.5526/ERDR-00000072 and FT-ICR-MS data (https://doi.org/10.5526/ERDR-00000084) are available from the University of Essex data repository. Sequence data are archived at the European Bioinformatics institute, http://www.ebi.ac.uk, under accession number PRJEB20754.

References

65. Zhou, J., Mopper, K. & Passow, U. The role of surface active carbohydrates in the formation of transparent exopolymer particles by bubble adsorption of seawater. *Limnol. Oceanogr.* **43**, 1860–1871 (1998).
66. Underwood, G. J. C., Fietz, S., Papadimitriou, S., Thomas, D. N. & Dieckmann, G. S. Distribution and composition of dissolved extracellular polymeric substances (EPS) in Antarctic Sea Ice. *Mar. Ecol. Prog. Ser.* **404**, 1–19 (2010).
67. Norman, L. et al. The role of bacterial and algal exopolymeric substances in iron chemistry. *Mar. Chem.* **186**, 148–161 (2015).
68. Grasshoff, K., Kremling, K. & Ehrhardt, M. (eds) *Methods of Seawater Analysis* 3rd edn (Wiley, 1999).
69. Knap, A., Michaels, A., Close, A., Ducklow, H. & Dickson, A. *Protocols for the Joint Global Ocean Flux Study (JGOFS) Core Measurements*, JGOFS Report No. 19, Reprint of the IOC Manuals and Guides No. 29, UNESCO 1994 (JGOFS, 1996).
70. Dubois, M., Gilles, K. A., Hamilton, J. K., Rebers, P. A. & Smith, F. Colorimetric method for determination of sugars and related substances. *Anal. Chem.* **28**, 350–356 (1956).
71. Decho, A. W. Microbial exopolymer secretions in ocean environments: their role(s) in food webs and marine processes. *Oceanogr. Mar. Biol. Annu. Rev.* **28**, 73–153 (1990).
72. Herborg, L.-M., Thomas, D. N., Kennedy, H., Haas, C. & Dieckmann, C. Dissolved carbohydrates in Antarctic sea ice. *Antarct. Sci.* **13**, 119–125 (2001).
73. Sutherland, I. Biofilm exopolysaccharides: a strong and sticky framework. *Microbiology* **147**, 3–9 (2001).
74. Dittmar, T., Koch, B. P., Hertkorn, N. & Kattner, G. A simple and efficient method for the solid-phase extraction of dissolved organic matter (SPE-DOM) from seawater. *Limnol. Oceanogr. Methods* **6**, 230–235 (2008).
75. Koch, B. P., Kattner, G., Witt, M. & Passow, U. Molecular insights into the microbial formation of marine dissolved organic matter: recalcitrant or labile? *Biogeosciences* **11**, 4173–4190 (2014).
76. Lechtenfeld, O. J. et al. The influence of salinity on the molecular and optical properties of surface microlayers in a karstic estuary. *Mar. Chem.* **150**, 25–38 (2013).
77. Marie, D., Partensky, F., Jacquet, S. & Vaulot, D. Enumeration and cell cycle analysis of natural populations of marine picoplankton by flow cytometry using the nucleic acid stain SYBR Green I. *Appl. Env. Microbiol.* **63**, 186–193 (1997).
78. Gasol, J. M., Zweifel, U. L., Peters, F., Fuhrman, J. A. & Hagström, Å. Significance of size and nucleic acid content heterogeneity as measured by flow cytometry in natural planktonic bacteria. *Appl. Environ. Microbiol.* **65**, 4475–4483 (1999).
79. Cosa, G., Focsaneanu, K. S., McLean, J. R. N., McNamee, J. P. & Scaiano, J. C. Photophysical properties of fluorescent DNA-dyes bound to single- and double-stranded DNA in aqueous buffered solution. *Photochem. Photobiol.* **73**, 585–599 (2001).
80. Smith, D. C. & Azam, F. A simple, economical method for measuring bacterial protein synthesis rates in seawater using ^{3}H-leucine. *Mar. Microb. Food Webs* **6**, 107–114 (1992).
81. Herndl, G. J. et al. Contribution of Archaea to total prokaryotic production in the deep Atlantic Ocean. *Appl. Environ. Microbiol.* **71**, 2303–2309 (2005).
82. Garneau, M.-E. et al. Hydrocarbon biodegradation by Arctic sea-ice and sub-ice microbial communities during microcosm experiments, Northwest Passage (Nunavut, Canada). *FEMS Microbiol. Ecol.* **92**, fiw130 (2016).
83. Caporaso, J. G. et al. QIIME allows analysis of high-throughput community sequencing data. *Nat. Methods* **7**, 335–336 (2010).
84. Quince, C., Lanzen, A., Davenport, R. J. & Turnbaugh, P. J. Removing noise from pyrosequenced amplicons. *BMC Bioinformatics* **12**, 38 (2011).
85. Edgar, R. C., Haas, B. J., Clemente, J. C., Quince, C. & Knight, R. UCHIME improves sensitivity and speed of chimera detection. *Bioinformatics* **27**, 2194–2200 (2011).
86. Wang, Q., Garrity, G. M., Tiedje, J. M. & Cole, J. R. Naïve Bayesian classifier for rapid assignment of rRNA sequences into the new bacterial taxonomy. *Appl. Environ. Microbiol.* **73**, 5261–5267 (2007).
87. Rognes, T., Flouri, T., Nichols, B., Quince, C. & Mahé, F. VSEARCH: a versatile open source tool for metagenomics. *PeerJ* **4**, e2584 (2016).
88. Bray, J. C. & Curtis, J. T. An ordination of the upland forest communities of southern Wisconsin. *Ecol. Monogr.* **27**, 325–349 (1957).